

# Theoretical Prediction and Experimental Determination of the Effect of Mold Characteristics on Temperature and Monomer Conversion Fraction Profiles During Polymerization of a PMMA-Based Bone Cement

Claudia I. Vallo

Institute of Materials Science and Technology (INTEMA), Universidad Nacional de Mar del Plata—National Research Council (CONICET), Av. Juan B. Justo 4302 (7600) Mar del Plata, Argentina

Received 29 October 2001; revised 19 February 2002; accepted 27 February 2002

**Abstract:** The present work is concerned with applications of a kinetic model for free-radical polymerization of a polymethylmethacrylate-based bone cement. Autocatalytic behavior at the first part of the reaction as well as a diffusion control phenomenon near vitrification are described by the model. Comparison of theoretical computations with experimental measurements for the temperature evolution during batch casting demonstrated the capacity of the proposed model to represent the kinetic behavior of the polymerization reaction. Temperature evolution and monomer conversion were simulated for the cure of the cement in molds made of different materials. The maximum monomer conversion fraction was markedly influenced by the physical properties of the mold material. The unreacted monomer acts as a plasticizer that influences the mechanical behavior of the cement. Hence, the same cement formulation cured in molds of different materials may result in different mechanical response because of the differences in the amounts of residual monomer. Standardization of the mold type to prepare specimens for the mechanical characterization of bone cements is recommended. Theoretical prediction of temperature evolution during hip replacement indicated that for cement thickness lower than 6 mm the peak temperature at the bone–cement interface was below the limit stated for thermal injury (50 °C for more than 1 min). The use of thin cement layers is recommended to diminish the risk of thermal injury; however, it is accompanied by an increase in the amount of unreacted monomer present in the cured material. © 2002 Wiley Periodicals, Inc. *J Biomed Mater Res (Appl Biomater)* 63: 627–642, 2002

**Keywords:** acrylic bone cements; computer simulations; batch casting; temperature evolution; residual monomer

## INTRODUCTION

Self-curing acrylic cement based on polymethylmethacrylate (PMMA) has a long history of application in orthopedic surgery, and a considerable body of data on its use is available.<sup>1</sup> It is well known that the exothermic nature of free-radical bulk polymerization together with the inferior heat transfer characteristics of polymers frequently leads to elevated cure temperatures. High temperature observed during polymerization has been considered the main adverse effect for clinical use of bone cements. In fact, the evaluation of the

peak temperature reached at the bone–cement interface has been the focus of much research.<sup>2–7</sup> Furthermore, it is generally accepted that a certain amount of residual monomer remains in the hardened material.<sup>8,9</sup> This is attributed to the fact that the vitrification phenomenon limits the degree of polymerization attained by the monomer.<sup>10–13</sup> The polymerization reaction progresses until the polymer–monomer mixture becomes a glass. At this stage the mobility of the reactive groups is hindered by the reduced mobility of the medium, and the diffusion of chemical reactants becomes a limiting step. Because of the diffusion control phenomenon a cessation of the reaction is observed, although the monomer conversion is not complete. The maximum conversion attained by the monomer depends on the cure temperature, however, a subsequent exposure of the sample to temperatures greater than the cure temperature results in further reaction. From a practical point of view, an important consequence arising

Correspondence to: Claudia I. Vallo, Institute of Materials Science and Technology (INTEMA), Universidad Nacional de Mar del Plata—National Research Council (CONICET), Av. Juan B. Justo 4302 (7600) Mar del Plata, Argentina (e-mail: civallo@fi.mdp.edu.ar)

Contract grant number: National Research Council (CONICET)

© 2002 Wiley Periodicals, Inc.

from the incomplete cure is the fact that as the unreacted monomer acts as a plasticizer and influences the mechanical properties of the cement.<sup>9,11–13</sup>

The purpose of this work was to investigate the batch casting process of a bone cement in order to predict the temperature evolution and the final monomer conversion for the cure in different type of molds. This study aims to elucidate whether the mold material influences the characteristics of the cured cement, particularly the degree of cure of the monomer. The cure temperature is determined by the relative rates of heat generation and of heat transfer. Thus, the kinetic analysis of the polymerization reaction is the essential step for a better understanding of the cure process. The polymerization reaction was followed by differential scanning calorimetry (DSC), which has been found to provide a convenient and useful method of monitoring the course of exothermic reactions.<sup>10,12,14</sup> Experimental details of the DSC technique used to monitor the polymerization of bone cements were reported elsewhere.<sup>10,12</sup> The method is based on the measurement of the rate at which heat is generated in an exothermic reaction. With the assumption that the heat generated by the reaction is proportional to the extent of reaction, the kinetic parameters can be obtained. Expressions for the rate of heat production were obtained from DSC measurement carried out at different temperatures. The objective of this approach is to obtain reasonably accurate and yet realistic kinetic expressions that can be used to solve the energy balance associated with any particular situation. The advantage of having a model able to predict the rate of reaction and, in turn, the rate of heat production lies in that it permit the calculation of the temperature progress as well as the monomer conversion. Thus, it is possible to calculate the degree of polymerization attained by the monomer and consequently the residual monomer content in the cured material. The capacity of the proposed model to describe the kinetic behavior of the polymerization reaction was assessed by comparison of theoretical prediction with experimental measurements for temperature evolution during the cure in rectangular and cylindrical molds. Theoretical computations were carried out to analyze the influence of the mold material on the maximum conversion attained by the monomer. Results of computations performed to predict peak temperatures reached during hip replacement are also presented.

## MATERIALS AND METHODS

### Materials

A commercial radiolucent bone cement, Subiton (Subiton, SRL, Argentina) was employed for this study. Each dose of surgical bone cement consists of an envelope with 40 g of acrylic powder and an ampoule with 20 g of liquid methyl methacrylate monomer. The liquid component is composed of 19.76 g methyl methacrylate monomer, 0.24 g *N,N*-dimethyl-*p*-toluidine, and 18–20 ppm hydroquinone. The solid

component is composed of 39.03 g poly(methyl methacrylate) and 0.97 g benzoyl peroxide.

### Temperature Evolution During the Cure in Molds

The temperature evolution during the polymerization of the resins was measured in both rectangular and cylindrical molds. The cement components were manually mixed according to the instructions of the manufacturers, and the mixture was poured into the molds. Rectangular molds consisted of two glass plaques spaced by rubber cords and held together with clamps. The thickness of the cement mantle was 4 and 8 mm. Cylindrical molds consisted of high-density polyethylene (HDPE) tubes of 10-mm internal diameters and 100-mm length, and polypropylene (PP) tubes of 6-mm internal diameter and 80-mm length.

Temperature changes during polymerization were followed by the insertion of thermocouples into the molds. Two thermocouples (Type J, Omega, accuracy  $\pm 0.1$  °C, temperature range 0–200 °C) were used to record temperature profiles in the center and at the internal mold wall. The thermocouples were connected to a data-acquisition system that registers values of temperature every 2 s. Measurements were carried out at two different ambient temperatures (25 and 15 °C) in order to study the influence of heat interchange with the surroundings on the peak temperature. The cement constituents were stored at ambient temperature for at last 24 h prior to mixing. After the experiments, the cured material was cut with a saw to verify by visual inspection the proper position of the thermocouple tips and to find any voids surrounding the thermocouples. All test were performed in triplicate.

### Theoretical Analysis

The heat generated by the exothermic polymerization of PMMA results in an increase of the temperature in the cement mass. The local temperature for a given time is related to the heat-production rate and the heat-transfer rate, as stated by the general conduction equation, which in Cartesian coordinate system is given by

$$\rho c_p \frac{\partial T}{\partial t} = \lambda \frac{\partial^2 T}{\partial x^2} + q'' \quad [\text{cal/cm}^3 \text{ min}], \quad (1)$$

where  $T$  is the temperature,  $x$  is the position, and  $t$  is the time. The cement properties involved are the thermal conductivity  $\lambda$ , the density  $\rho$ , and the specific heat per unit mass  $c_p$ . Here  $q''$  is the rate of heat generation per unit volume. A rectangular mold having very large dimensions in the  $y$  and  $z$ -directions was assumed, so that the temperature gradient is significant in the  $x$  direction only. If the thermal conductivity is taken as constant, Eq. (1) reduces to

$$\frac{\partial T}{\partial t} = \alpha \frac{\partial^2 T}{\partial x^2} + \frac{q''}{\rho c_p} \quad [^\circ\text{C/min}], \quad (2)$$

where  $\alpha$  is the thermal diffusivity defined by  $\lambda/\rho c_p$ .

For the cure of the resin in cylindrical molds, the partial differential equation in cylindrical coordinate system is

$$\frac{\partial T}{\partial t} = \alpha \left( \frac{\partial^2 T}{\partial r^2} + \frac{1}{r} \frac{\partial T}{\partial r} \right) + \frac{q''}{\rho_p} \quad [^\circ\text{C}/\text{min}], \quad (3)$$

where  $r$  is the radius of the mold. Similarly to the case of rectangular molds, it was assumed that the cylinder is long enough so that the temperature gradient is significant in the  $r$  direction only.

In order to solve Eq. (2) or (3) for the temperature  $T$  as a function of the position  $x$  (or  $r$ ) and the time  $t$ , it is necessary to know the rate of heat production due to the polymerization reaction,  $q''$ . A kinetic model previously developed was used to calculate the rate of heat production as a function of time and temperature. Details of the model were reported elsewhere<sup>10</sup> and are briefly described here. The polymerization reaction can be divided into two steps. In the first step the reaction exhibits autocatalytic behavior as follows:

$$\frac{dp}{dt} = k(T)p(1-p), \quad (4)$$

where  $dp/dt$  is the reaction rate,  $k(T)$  is the kinetic rate constant, which depends on temperature, following the Arrhenius relationship,  $p$  is the fraction of reacted monomer and  $(1-p)$  is the fraction of unreacted monomer. The weight fraction of unreacted monomer based on the total mass is

$$w_f = \frac{1}{3}(1-p),$$

where the factor  $1/3$  represents the initial mass of monomer divided by the initial total mass.

In the second part of polymerization the reaction rate is described by the following relationship:

$$\frac{dp}{dt} = k^*p(1-p)^2, \quad (5)$$

where

$$k^* = k(T) \frac{(p_u - p_m)}{(1 - p_m)(p_u - p_m)}. \quad (6)$$

$k^*$  is the constant rate, which depends on both cure temperature and monomer conversion,  $p_m$  is the conversion at the point of maximum reaction rate, and  $p_u$  is the maximum conversion attained by the monomer. Both  $p_u$  and  $p_m$  are linear functions of the cure temperature. If the dependences of  $k$ ,  $p_u$ , and  $p_m$  with the cure temperature are known, it is possible to calculate the reaction rate and the proportion of reacted monomer as a function of time and cure temperature.

The dependence of  $k$ ,  $p_m$ , and  $p_u$  with temperature is given by the following expressions:<sup>10</sup>

$$k(T) = 8.04 \cdot 10^7 \exp[-4.8 \times 10^3/T (^\circ\text{K})],$$

$$p_m = 0.236 + 0.003 T (^\circ\text{C}),$$

$$p_u = 0.583 + 0.004 T (^\circ\text{C}).$$

The kinetic model was incorporated into the energy balance, and the local temperature and monomer conversion as a function of time were computed. The problem can then be described by the outlined differential equations along with one initial and two boundary conditions (BC). The following boundary conditions and time condition were used.

**Time Condition.** The mixture and the mold are initially ( $t=0$ ) at the uniform temperature  $T_i$ , and are exposed to air at ambient temperature  $T_{\text{amb}}$ .

#### Boundary Conditions ( $t>0$ ).

BC1: In the center of the mold  $\partial T/\partial x = 0$  (or  $\partial T/\partial r = 0$ ) (symmetry condition)

BC2: The system is surrounded by air of a known temperature  $T_{\text{amb}}$ .

The external surface of the mold is exposed to free convective airflow. Energy is carried or convected away by the air and at the solid–fluid interface the energy transport by the mechanism of convection is given by  $q = h A (T_s - T_{\text{amb}})$ . Here  $h$  is the heat-transfer coefficient,  $A$  is the area normal to the direction of the heat flux, and  $(T_s - T_{\text{amb}})$  is difference between the temperature at the interface  $T_s$  and that in the air. The heat-transfer coefficient was evaluated from standard empirical correlations.<sup>14</sup> The energy balance was solved by a numerical scheme that used the Crank–Nicolson finite-difference method coupled with the standard fourth-order Runge–Kutta algorithm to give local temperature and monomer conversion fraction conversion profiles.

## RESULTS AND DISCUSSION

### Kinetic Model

The temperature reached during the cure of a PMMA-based bone cement depends on the balance between the rate of heat production and the rate of heat transfer within the medium. The first step for the evaluation of the rate of heat production is to obtain adequate information about the reaction kinetics.

The polymerization of a bone cement involves the transformation of a viscous paste into a solid mantle as a result of the chemical reaction between active groups present in the system. Differential scanning calorimetry (DSC) is widely used to characterize polymeric materials. Because exothermic peak due to cure reaction is accurately detected, DSC is a

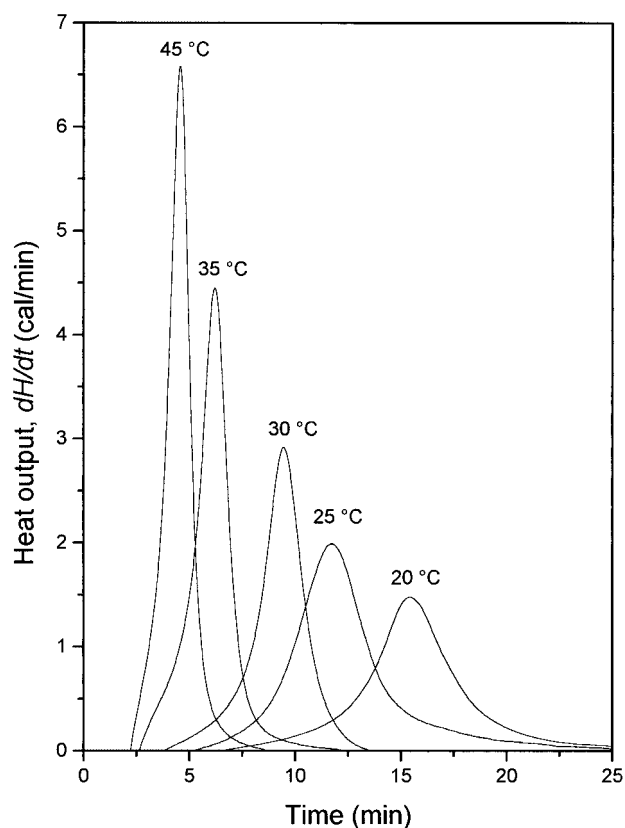


Figure 1. DSC thermograms of rate of heat production as a function of time for different cure temperatures.

suitable technique to measure the heat released during the cure of the cement. A unique feature of the use of the DSC is the quantitative nature of the thermal data generated by the technique. Because the heat produced is proportional to the number of monomer units reacted, the degree of polymerization can be measured directly. Figure 1 shows DSC curves of the rate of heat generated,  $dH/dt$ , versus time at different cure temperatures. The polymerization starts after the inhibitor is consumed. As the monomer conversion increases the reaction rate increases and reaches a maximum rate that is characteristic of autocatalytic reactions. The observed autocatalytic behavior and the influence of cure temperature in the first part of the reaction are described by the expression (4). Finally, the reaction rate decays to zero because of the transition of the polymer–monomer system from a viscous liquid to a glassy solid. The decrease of  $k^*$  with the extent of the reaction given by the expression (5) takes into account the diffusion control effects presents near vitrification.

The reaction rate  $dp/dt$  was determined from DSC thermograms according to

$$\frac{dp}{dt} = \frac{1}{\Delta H_{\text{tot}}} \left( \frac{dH}{dt} \right), \quad (7)$$

where  $\Delta H_{\text{tot}}$  represents the heat generated per mol of reacted monomer (56.9 kJ/mol).<sup>15</sup> Hence, to express the experimental

results in terms of the extent of reaction  $p$ , the DSC curves, normalized with respect to  $\Delta H_{\text{tot}}$  and sample weight, were integrated as a function of time. The maximum monomer conversion fraction  $p_u$  is proportional to the total area under the DSC thermograms. As it is seen in Figure 1 the area under the exothermic peak and therefore the maximum monomer conversion  $p_u$  increases with the cure temperature. Measurements of  $p_u$  as a function of the cure temperature by DSC and gas chromatography were reported elsewhere,<sup>12</sup> and the results are presented in Figure 2. For a given temperature the polymerization progresses until the mixture polymer–monomer becomes a glass. When vitrification is attained even small molecules have extremely low mobility; hence, the diffusion of chemical reactants becomes a limiting step. A cessation of the reaction is observed, although the reaction is not complete, and for practical purposes the reaction rate is zero in the normal reaction-time scale. When the reaction is quenched by vitrification a subsequent exposure to temperatures greater than the cure temperature results in further reaction.<sup>10–13</sup> However, in absence of an external heat source the monomer reaches a maximum conversion value  $p_u$ , which is related with the cure temperature by the vitrification curve (Figure 2).

Equations (4) and (5) were solved by the standard fourth-order Runge–Kutta algorithm to give reaction rate and fraction of reacted monomer as a function of time. Figure 3 gives plots of experimental results along with computed values for

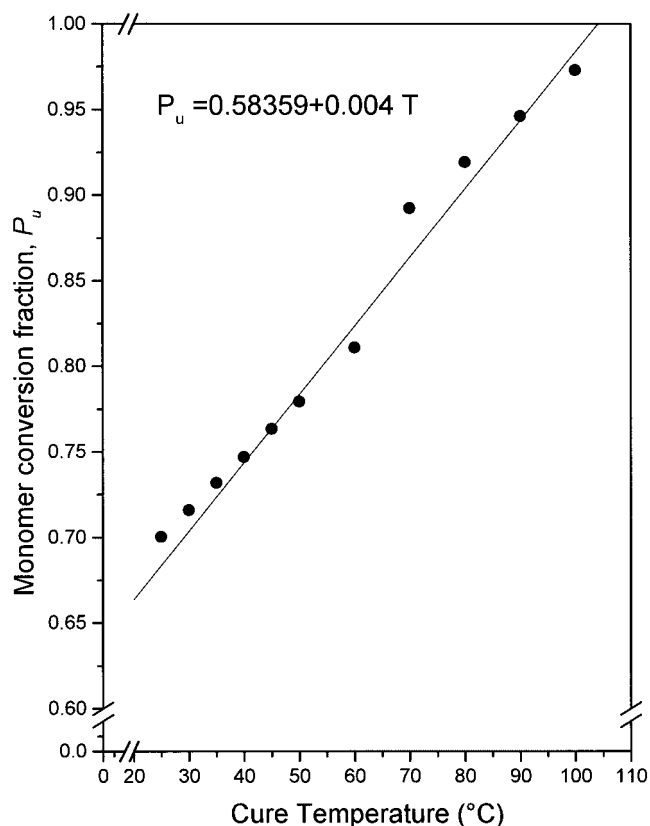
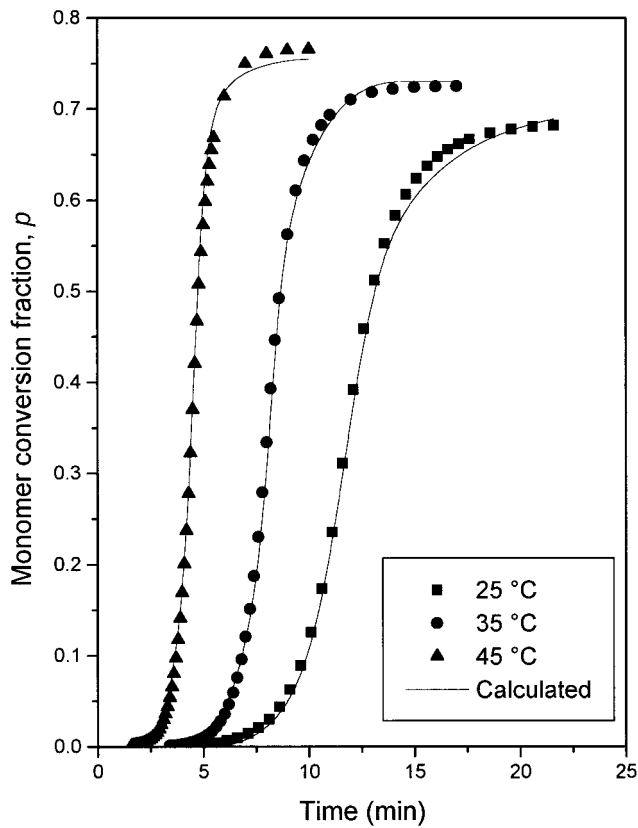


Figure 2. Maximum monomer conversion fraction versus cure temperature.



**Figure 3.** Experimental results (from Reference 10) and theoretical computations for monomer conversion fraction versus time at different cure temperatures.

runs carried out at different cure temperatures. The agreement between predicted and experimental results is found to be satisfactory and to lend support to the expressions used to calculate the reaction rate.

It is worth noting that although a vast amount of literature is available on the cure reaction of industrial PMMA, this is not directly applicable to bone cements. Because commercial bone cements consist of a complex mixture of radical initiator, modifiers, and inhibitors, it is very difficult to obtain the characteristics of the cure reaction of acrylic bone cements without detailed and extensive chemical analysis. One of the problems lies in the fact that it is difficult to establish the

amount of inhibitor in commercial resins, because it is incorporated during the manufacture of the prepolymer, and is consumed during the storage of the resin. This means that the resin evolves, and the amount of inhibitor is variable over time. On the other hand, though the decomposition constants of the peroxides are tabulated, they have been obtained in conditions different from those in which the peroxide decomposes during the curing. Alternatives to the fundamental models are empirical or phenomenological models like the model formulated in Eqs. (4) and (5). This kind of analysis is unfortunately accompanied by the unavoidable loss of knowledge about the path of reaction. However, for practical purposes, it is convenient to adopt an engineering approach formulating an empirical model to describe the kinetic behavior and to verify the phenomenological model with different experimental results.

#### Experimental Measurements for Batch Casting

The kinetic model described above was used to predict the progress of temperature and monomer conversion during the cure in molds of different sizes and geometries. The rate of heat production  $q''$  is related to the reaction rate by the following relationship:

$$q'' = \frac{L}{L + P} \Delta H_{\text{tot}} \rho \frac{dp}{dt}, \quad [\text{cal/cm}^3 \text{ min}] \quad (8)$$

where  $\rho$  is the cement density,  $L$  is the mass of liquid monomer, and  $P$  is the mass of prepolymerized powder. Thus, the progress of temperature and monomer conversion can be calculated by solving the energy balance coupled with the kinetic model for the calculus of  $q''$ . Computations were carried out in rectangular and cylindrical coordinates given by Eqs. (2) and (3), respectively, coupled with Eqs. (4) and (5). The numerical values used for the physical and thermal properties of the cement and mold material are shown in Table I. It was assumed that the temperature rise was not so large that the temperature dependence of the physical properties needed to be considered. At the mold–air interface the heat loss was calculated as  $h(T_s - T_{\text{amb}})$ . The heat-transfer coefficients, evaluated under free convective airflow,<sup>14</sup> were  $3 \times 10^{-4} \text{ cal/s cm}^2 \text{ }^\circ\text{C}$  for rectangular plaques and  $4.7 \times 10^{-4}$

**TABLE I.** Physical Properties of the Selected Materials (HDPE: High density Polyethylene, PTFE: Polytetrafluoroethylene, PP: Polypropylene). The Values of the Physical Properties of Bone cement were Taken from References 2 and 4

Material	$\rho$ (g/cm <sup>3</sup> )	$C_p$ (J/g °C)	$\rho C_p$ (10 <sup>-6</sup> ) (J/m <sup>3</sup> °C)	$\lambda$ (J/m s °C)	$\alpha$ (10 <sup>7</sup> ) (m <sup>2</sup> /s)
Bone cement	1.19	1.46	1.75	0.17	0.96
Glass	2.7	0.84	2.26	0.76	3.30
HDPE	0.96	2.30	2.21	0.50	2.30
PTFE	2.16	1.04	2.26	0.24	1.10
PP	0.9	1.92	1.71	0.12	0.68
Aluminum	2.7	0.88	2.34	200	859
Steel	7.8	0.50	3.93	15.26	39
Bone	2.6	1.17	3.05	0.29	0.95



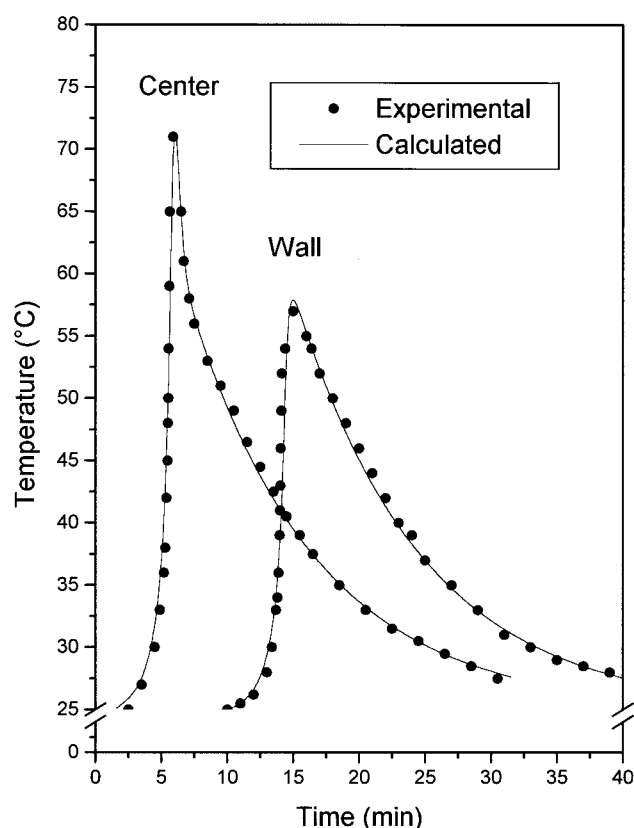


**Figure 4.** Temperature evolution during the cure in a rectangular glass mold for a cement thickness of 4 mm.

and  $3.6 \times 10^{-4}$  cal/s cm<sup>2</sup> °C for cylindrical molds of 6- and 10-mm diameter, respectively. The capacity of the proposed model to predict the temperature–time history during polymerization was assessed by comparison of theoretical computations with experimental results. Experimental measurements of the temperature evolution during the curing were carried out in rectangular and cylindrical molds as described earlier. Figures 4 and 5 give plots of the temperature–time history in the center and at the wall of rectangular molds. The wall temperature profile was shifted 10 min with respect to the center temperature profile to make the plots clearer. A good fit was obtained between experimental and theoretical results, confirming the procedure used for the calculus of  $q''$ . A sharp temperature rise caused by the reaction exotherm during the initial fast free-radical polymerization is observed. At this stage, the rate of heat transfer by conduction is much lower than the rate of heat production; therefore, a considerable part of the energy liberated is accumulated into the system. As the mixture approaches vitrification the reaction rate and therefore the rate of heat production decreases. After that point the reaction is diffusion controlled and the rate of heat production is negligible compared with the rate of heat transfer. Consequently, the local temperature decreases rapidly. For the material cured near the wall the temperature changes are moderated by heat exchange throughout the mold wall; therefore, the peak temperature at the wall is lower than that in the center. Finally, concluding the profile, there is a

period during which heat is transferred out from the reacted polymer throughout the wall. Figures 6 and 7 give the evolution of the temperature in the center of cylindrical molds along with the theoretically predicted profiles. In results presented in Figure 7 the initial temperature of the mixture and the liquid to powder ratio (L/P) were varied with respect to that used in clinical practice. However, these experiments yield an alternative procedure to corroborate the proposed model. Because the amount of inhibitor present in the mixture increases with the L/P ratio, the initiation of the polymerization is delayed in samples having a higher proportion of monomer. On the other hand, the amount of heat released is related to the L/P ratio by the relationship given in Eq. (8). Therefore, the peak temperature increases with the increase in the L/P ratio. The agreement between experimental results and theoretical predictions presented in Figures 6 and 7 is satisfactory, giving additional confirmation of the ability of the model to reproduce the kinetic behavior of the formulation studied.

From results presented in Figures 4–7 it emerges that the size and geometry of the mold control the relative rates of heat generation and heat transfer, and consequently the temperature evolution during polymerization. On the other hand, the cure temperature determines the final monomer conversion, because the vitrification phenomenon limits the extent of reaction. As was shown in Figure 2, the higher the cure temperature, the higher the monomer conversion. This means

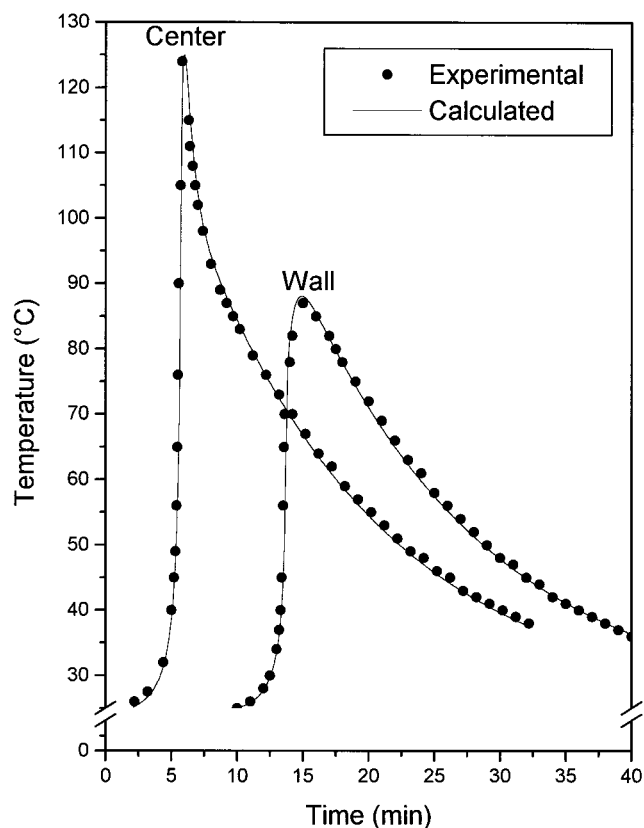


**Figure 5.** Temperature evolution during the cure in a rectangular glass mold for a cement thickness of 10 mm.

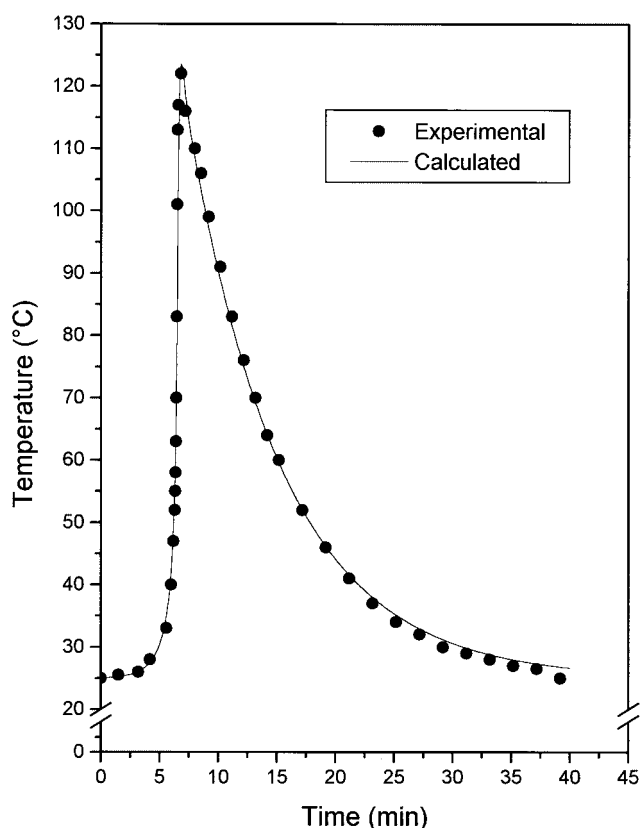


**Figure 6.** Temperature evolution in the center of the mold during the batch casting in a cylindrical HDPE mold. The diameter of the mold is 10 mm.

that differences in monomer conversion arising from differences in mold volume are expected to occur.

The maximum temperature expected during polymerization is the temperature reached under adiabatic conditions. When the system is perfectly insulated and heat losses are neglected, Eq. (2) becomes

$$\frac{dT}{dt} = \frac{\Delta H_{\text{tot}}}{3cp} \frac{dp}{dt} \quad (9)$$

Assuming an initial temperature of 25 °C and complete monomer conversion, Eq. (9) results in a maximum temperature value equal to 155 °C. Any temperature measured below this value is attributed to heat losses or incomplete monomer conversion. The maximum temperature measured by previous workers<sup>4</sup> during the cure under adiabatic conditions was below the value resulting from Eq. (9), which confirms that the extent of the reaction was limited by the vitrification process.

The practical consequence of the cure behavior of the cement lies in the fact that the unreacted monomer present in the hardened material acts as a plasticizer, which influences its mechanical behavior.

#### Model Prediction for Batch Casting

Although the effect of the volume of the mold on the peak temperature has been widely reported,<sup>2,4</sup> the influence of the

material from which the mold is made on the evolution of temperature and monomer conversion has not received the same attention. On the basis of the agreement between theoretical predictions and experimental results presented above, theoretical computations were carried out to predict the progress of temperature and monomer conversion during the cure in molds of different materials. For rectangular molds the selected mold materials were steel, aluminum, and PTFE. The wall thickness of the mold was set equal to 2 mm, and the cement thickness was varied in the range of 2–10 mm. For cylindrical molds, the wall thickness of the mold was set equal to 2 mm and the diameter was 6 mm. Computations were carried out for molds made of steel, PTFE, and polypropylene (PP). These sizes and mold materials were selected because they are commonly used in the preparation of samples for mechanical characterization of bone cements.

Figures 8 (a)–8(c) show the predicted temperature (left axis) and monomer conversion (right axis) profiles calculated for the cure in rectangular molds. The plots shown in Figure 8 reveal the marked influence of the thermal characteristics of the material in contact with the acrylic mass upon the final conversion attained by the monomer. The acrylic cement is a relatively poor conductor (see Table I), and therefore heat escapes less easily from the center. Heat transfer from the cement mass is governed essentially by the processes of conduction through the wall of the mold and free convection

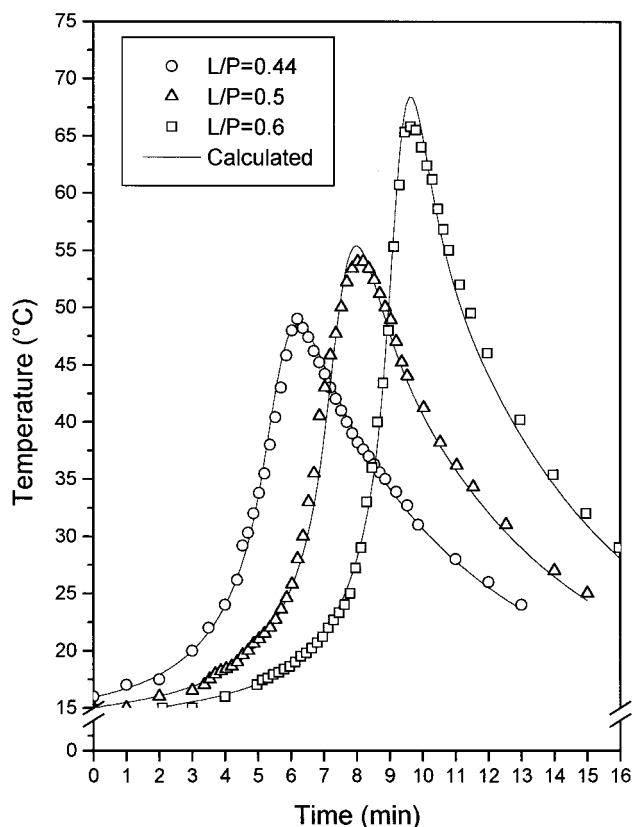


**Figure 7.** Temperature evolution in the center of the mold during the batch casting in cylindrical PP molds. The diameter of the mold is 6 mm and the samples have different liquid to powder ratio (L/P).

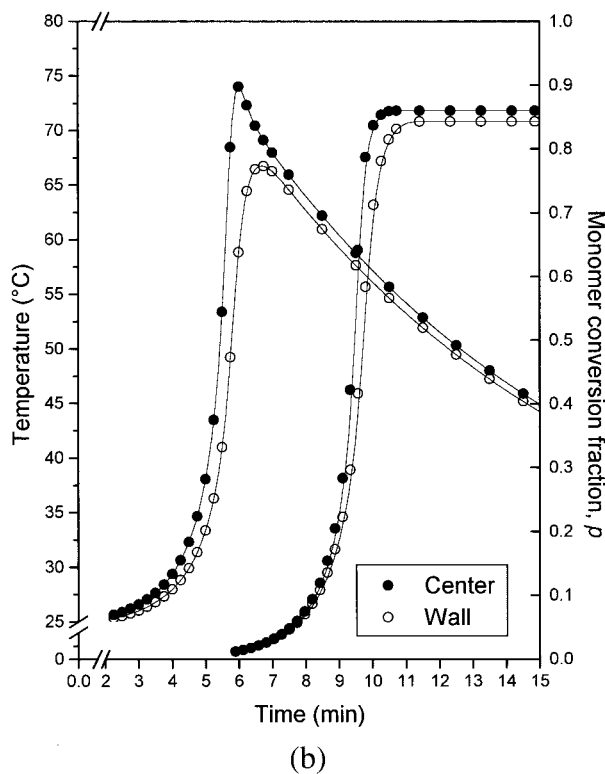
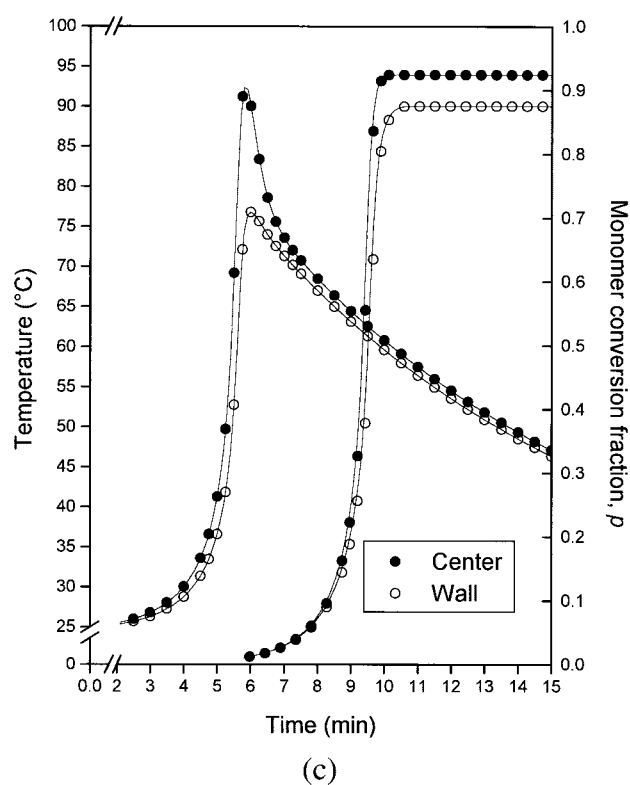
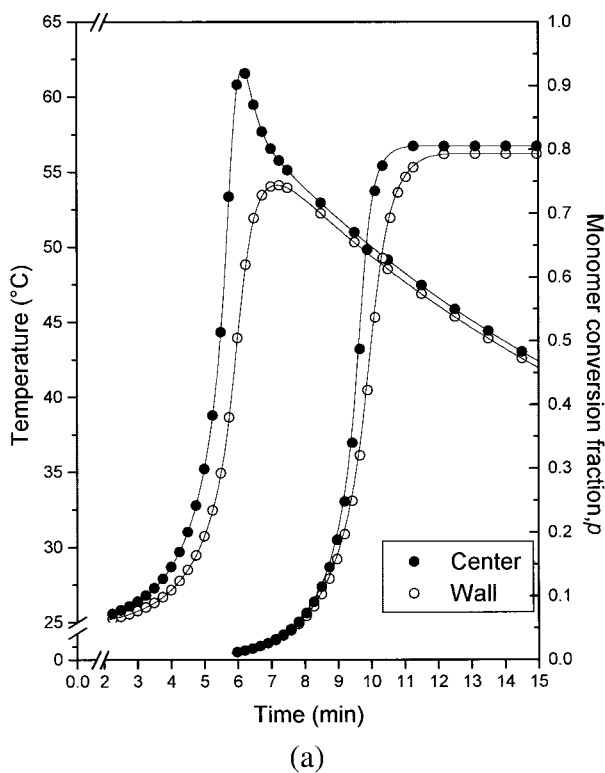


**Figure 8.** Temperature and monomer conversion fraction for the cure in rectangular steel molds. The thickness of the cement is 4 mm. (a) Steel mold, (b) aluminum mold, (c) PTFE mold.

at the solid-air interface. The temperature at the mold-cement interface is inversely related to the product of the density and the specific heat at the interface, that is, the heat capacity  $\rho c_p$ . Steel displays a  $\rho c_p$  value almost twice the value for aluminum or PTFE. Therefore, a 1 °C increase of tem-

perature for the steel mold requires about twice the heat generated compared with aluminum or PTFE molds. As a result, the temperature reached at the interface during the cure in steel mold is lower than that in aluminum or PTFE molds. In addition, the lower temperature at the steel mold-cement



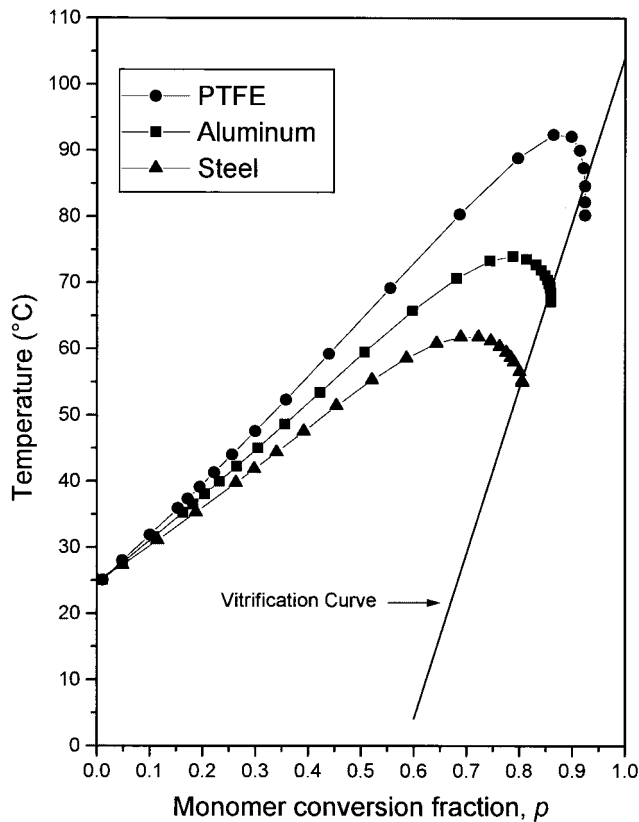


**Figure 9.** Evolution of the temperature and monomer conversion fraction in the center of the cement mass during the batch casting in the molds depicted in Figure 8.

interface promotes heat losses through the wall, which results in an overall lower cure temperature and consequently in a lower monomer conversion. The theoretical results presented in Figure 8 are in agreement with experimental measurements reported by previous workers on temperature evolution during the cure of a bone cement in aluminum and PTFE molds.<sup>2</sup>

Results presented in Figure 8 were plotted as monomer conversion versus temperature in Figure 9. The vitrification curve is shown in the same plot, and the curves correspond to the cure in the center of the mold. The temperature evolution in the cement is determined by the physical properties of each mold, particularly the  $\rho c_p$  value, as stated by the energy balance. As the mixture approaches the vitrification curve, the cement temperature decreases because of the drop in the rate of heat production. Finally, the polymerization ceases for an incomplete monomer conversion, giving as a result a cured material that contains a certain amount of unreacted monomer.

The relative rates of heat generation and heat transfer at any point within the cement determine the value of the local temperature. Figures 10(a) and 10(b) show the progress of the temperature across the thickness for the cure in steel and PTFE molds. The temperatures profiles correspond to the initial part of the reaction until the maximum temperature in the center of the mold was reached. It is observed that the

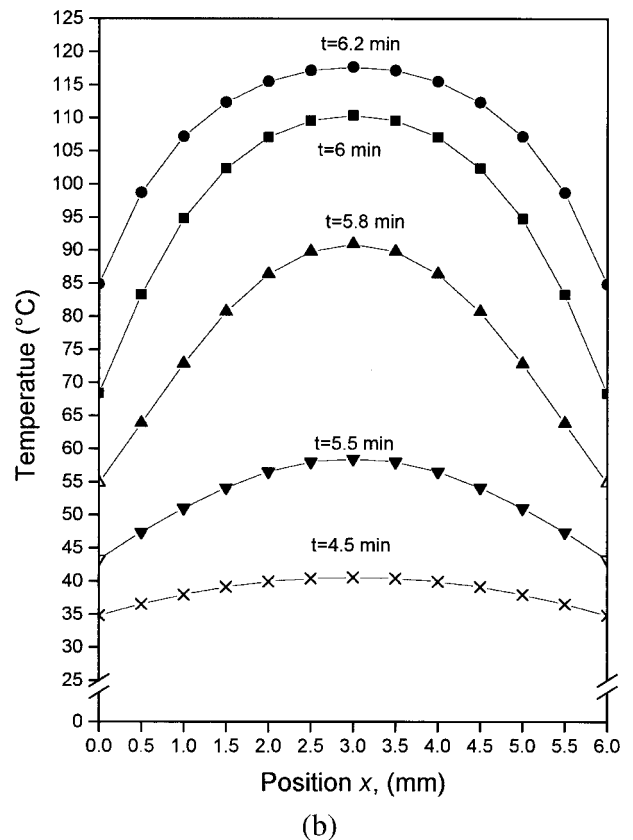
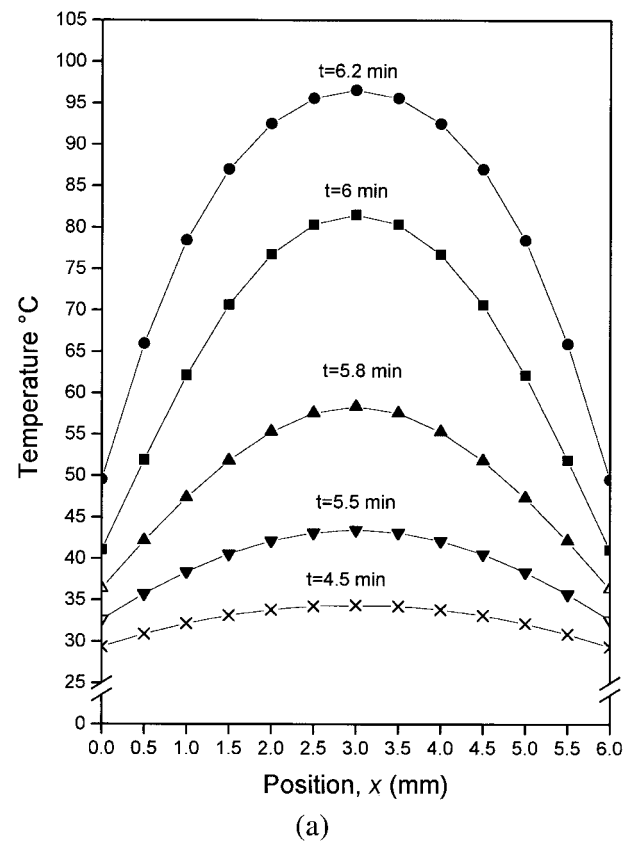


**Figure 10.** Temperature profiles for the cure in a rectangular molds. The thickness of the cement is 6 mm. (a) Steel mold, (b) PTFE mold.

cement polymerized in the steel mold displayed quite different temperature profile across the thickness compared with the cement cured in the PTFE mold. As discussed before, during the cure at low temperatures the polymerization reaction is not completed, and the system reaches a final value of the extent of reaction that is an increasing function of the cure temperature. Thus, a gradient of cure temperature gives as a result a gradient of monomer conversion. Figures 11(a) and 11(b) depict the gradient of final monomer conversion across the thickness for cements cured in molds of steel and PTFE of different thickness. The physical properties of the mold determine the temperature evolution across the cement, which, in turn, determines the local monomer conversion. This is seen more clearly in Figure 12, which shows the average weight percent of unreacted monomer present in the cured cement as a function of the cement thickness. The comparison of samples having the same thickness reveals the marked influence of the mold material on the feature of the cured material. For example, for a thickness equal to 4 mm, the amount of unreacted monomer present in the cement cured in the steel mold is about two times higher than that in the cement cured in the PTFE mold. Results presented in Figure 12 are in agreement with experimental results reported by Linder et al.<sup>8</sup> on measurements of monomer leakage from Simplex-P bone cement. The authors placed cement samples of different sizes into 30 ml of distilled water and measured the monomer leakage by gas chromatography. Comparison of the amount of leached-out monomer from samples having a same surface area but different thickness reveals that the weight percent of monomer present in samples of 1-mm thickness was about four times higher than that in samples of 5-mm thickness. The results of the Linder et al.<sup>8</sup> study thus provide verification of the present theoretical predictions for the influence of the cement thickness on the degree of monomer conversion.

Figures 13(a) and 13(b) show the predicted temperature for the cure in cylindrical molds. Similarly to the results presented above, a marked influence of the physical properties of the mold upon the evolution of the temperature during polymerization and consequently on the maximum monomer conversion is observed. Table II shows the percentage of unreacted monomer in the cured material averaged across the diameter.

All calculations presented in Figures 8–13 were performed by setting a temperature of 25 °C as initial and boundary conditions. However, it is interesting to evaluate the influence of the initial temperature of the mixture and the ambient temperature on the cure behavior of the cement. Figures 14(a) and 14(b) show the effect of changing the initial temperature of the mixture and the ambient temperature from 25 to 10 °C on the peak temperature and monomer conversion. It is seen that prechilling of the components at 10 °C before mixing while the cure is carried out at an ambient temperature of 25 °C reduces the peak temperature in about 10 °C and slightly reduces the final monomer conversion. This result is in agreement with experimental measurements of peak temperature for Simplex-P, CMW1, and Palacos R

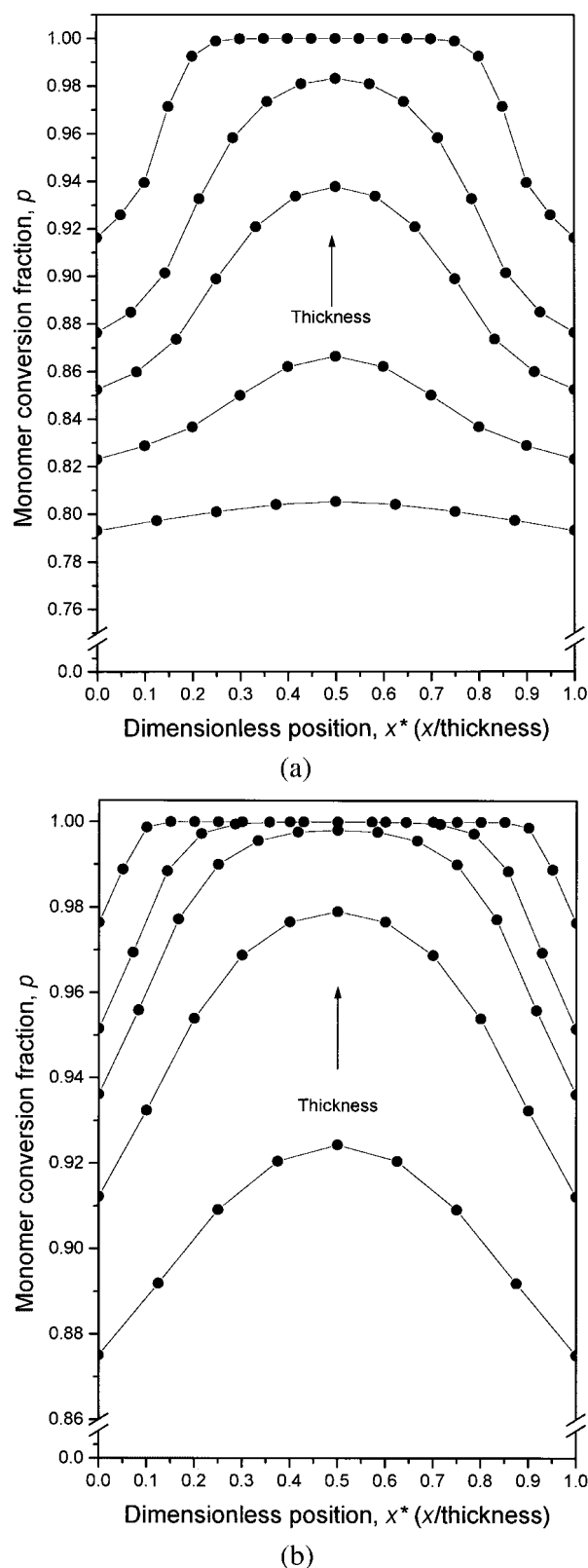


**Figure 11.** Final monomer conversion fraction profiles for the cure in a rectangular molds. The curves correspond to cement thickness from bottom to top equal to 4, 5, 6, 7, and 10 mm. The actual position is calculated by dimensionless position  $\times$  thickness. (a) Steel mold, (b) PTFE mold.

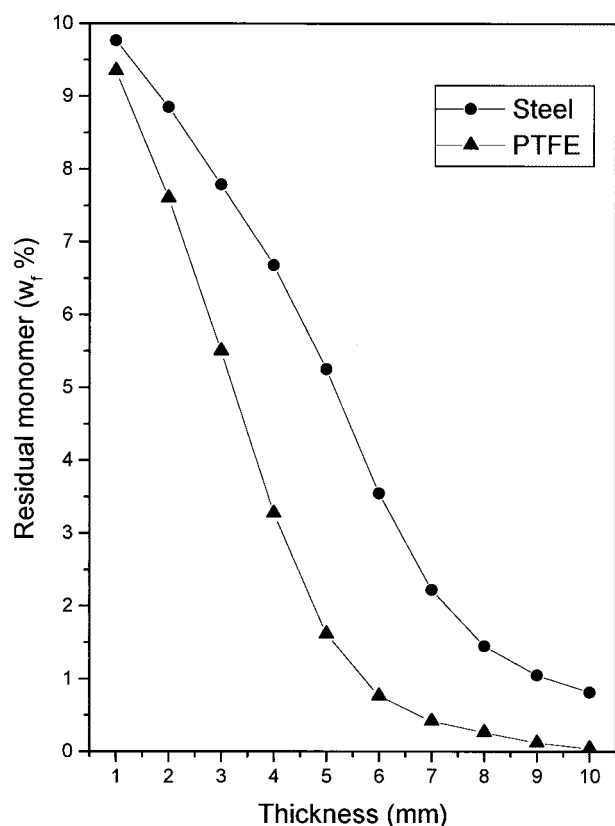


**Figure 12.** Weight percent of residual monomer as a function of the cement thickness after the cure in rectangular steel and PTFE molds. The values were averaged across the cement thickness.

bone cements reported by Wang et al.<sup>16</sup> High-viscosity Palacos R was prechilled to 4 °C before mixing, while the other two brands were mixed at room temperature (22–23 °C). Peak temperatures of 122 °C were recorded in Simplex-P and CMW1 but 107 °C for Palacos R. Because the cements display a relatively low heat capacity the peak temperature and consequently the monomer conversion are not markedly reduced by changing its initial temperature. However, the influence of the ambient temperature is much more marked. For samples cured at 10 °C the monomer reaches a final conversion of about 70%, which corresponds to a residual monomer content of 23 wt%. The predicted increase in the monomer content arisen from a low cure temperature is expected to influence the mechanical behavior of the cement, which is in accord with experimental measurements reported by Swenson et al.<sup>4</sup> The authors cured a cement in an 8 °C environment and measured peak temperatures of 13, 18, and 41 °C for molds of 7.5-, 10-, and 20-mm diameter, respectively. Fatigue test of the samples showed a 45% reduction in fatigue strength, which was attributed to an incomplete cure

of the resin. On the other hand, De Wijn<sup>17</sup> prepared incompletely cured samples by adding a polymerization inhibitor to the liquid component of a bone cement. Results of mechanical tests of the cement revealed a decrease of 50% in its compressive strength. Similarly, results reported in previous works<sup>11–13</sup> showed that samples containing unreacted mono-

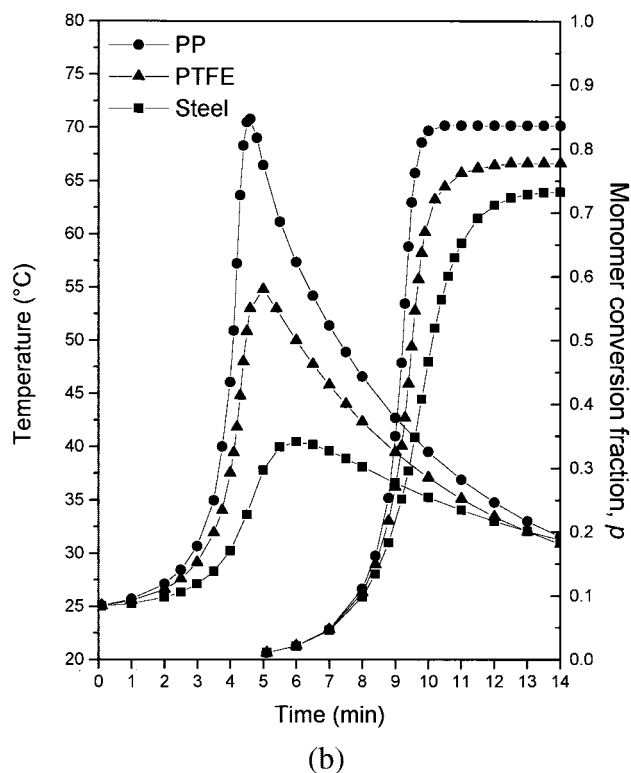
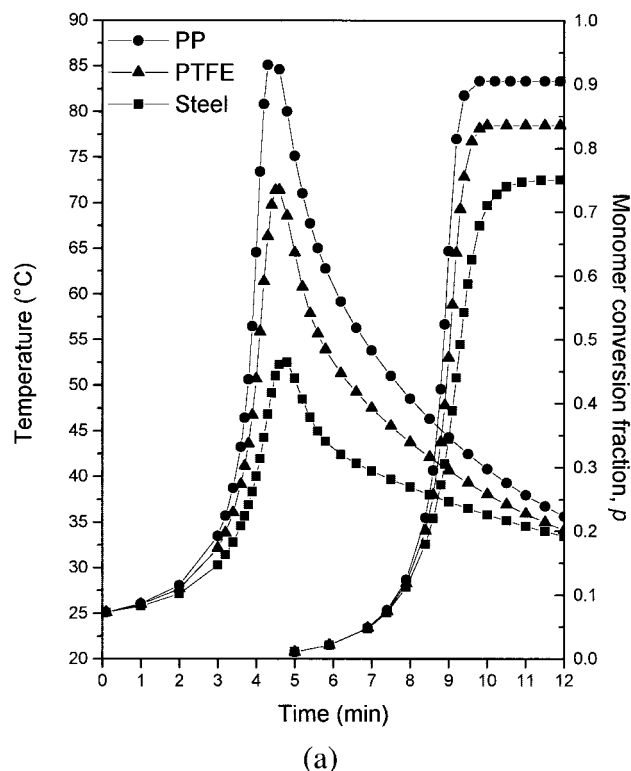


**Figure 13.** (a) Temperature and monomer conversion fraction computed in the center of cylindrical molds of 6 mm diameter. (b) Temperature and monomer conversion fraction computed at the wall of cylindrical molds of 6-mm diameter.

**TABLE II. Monomer Conversion Fraction and Weight Percent of Residual Monomer Content in 6-mm-Diameter Cylindrical Molds. The Values were Averaged Across the Diameter**

Mold Material	$p$ (%)	$w_f$ (%)
Steel	75	8.3
PTFE	83	5.7
PP	87	4.3

mer display lower yield stress and higher fracture toughness compared with samples free of unreacted monomer.

The results presented in Figures 8–14 show that as a result of the balance between the rate of heat production and the rate of heat transfer, samples cured in molds of different materials or different sizes reach different ultimate monomer conversions. This feature has important consequences with regard to the mechanical characterization of the cement because the monomer acts as a plasticizer. Hence, the same cement formulation cured in molds of different materials or sizes may result in different mechanical response. The conversion attained by the monomer and in turn the amount of unreacted monomer present in the cured material is related to the cure temperature. The higher the cure temperature, the lower the amount of unreacted monomer. As was said previously, the monomer acts as a plasticizer; consequently, the mechanical behavior of the cement is influenced by the cure temperature.

#### Model Predictions for Hip Replacement

Computer simulation for a hip replacement was carried out in order to evaluate peak temperatures at the bone–cement interface during polymerization, as well as monomer content after curing. As was shown previously, the temperatures reached during polymerization are conditioned by the physical properties of the surrounding material, the initial temperature of the system, the ambient temperature, and the cement thickness. On the other hand, the temperature at the mold–cement interface is particularly controlled by the heat capacity of the mold. Hence, the influence of these variables on peak temperatures and monomer conversion was analyzed.

The model for the femoral component consisted of a 10-mm-diameter steel stem surrounded by a layer of bone cement all embedded in cancellous bone. The thickness of the bone was set equal to 7 mm and the thickness of the cement varied from 2 to 8 mm. The ambient temperature was set equal to 25 °C and the initial temperature of the metal stem, bone cement, and bone were set equal to 25 °C. The initial bone temperature was selected considering results reported by Reckling et al.<sup>3</sup> on the measurement of the bone–cement interface temperature during total joint-replacement procedures. Experimental measurements showed that because the surgical field had been exposed to room temperature during the operation, the initial bone temperature was in the range 24–28 °C. The thermal conductivity of the bone depends on the bone mineral volume fraction. Experimentally measured values reported in the literature are  $7 \times 10^{-4}$  cal/cm s °C for hydrated cancellous bone,<sup>18</sup>  $5.45 \times 10^{-3}$  cal/cm s °C for liv-

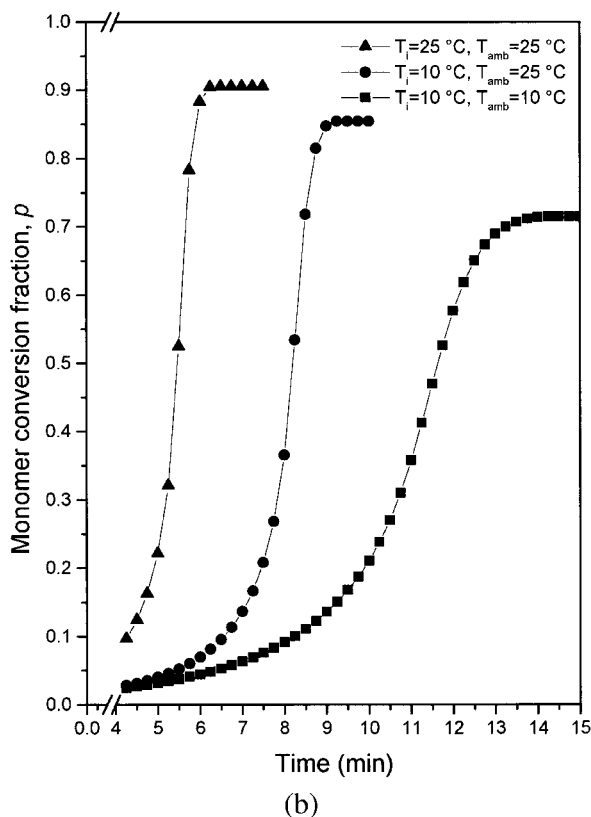
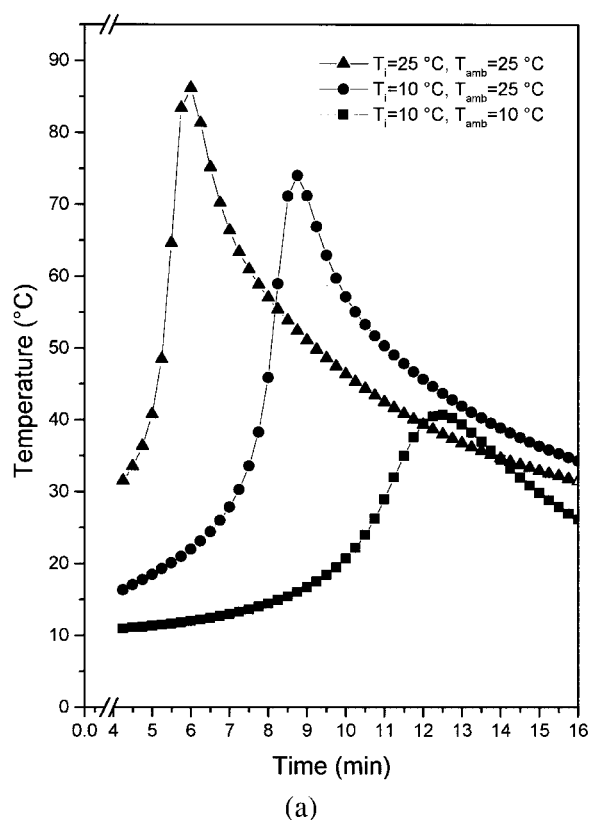


**Figure 14.** (a) Influence of the initial temperature of the mixture ( $T_i$ ) and ambient temperature ( $T_{amb}$ ) on the peak temperature for the polymerization in cylindrical PP molds of 6-mm diameter. (b) Influence of the initial temperature of the mixture ( $T_i$ ) and ambient temperature ( $T_{amb}$ ) on the monomer conversion fraction for the polymerization in cylindrical PP molds of 6-mm diameter.

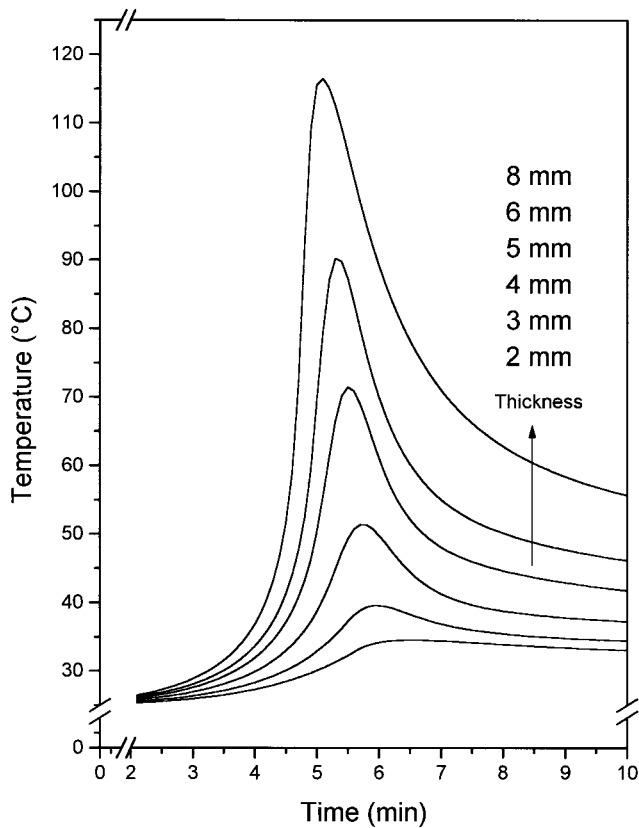


**Figure 15.** Temperature evolution in the center of the cement as a function of the cement thickness calculated for the femoral component in a hip replacement.

ing bovine compact bone<sup>19</sup> and  $8.5 \times 10^{-3}$  cal/cm s °C for hydrated human compact bone.<sup>20</sup> In order to obtain conservative values for the temperature at the bone–cement interface, the lower thermal conductivity was used in the present simulation (Table I), and the heat transfer between the bone surface and the surroundings was accounted for by free convection. The value used of the coefficient of heat transfer calculated for a free convective air flow was  $4.7 \times 10^{-4}$  cal/cm s °C. Differently from results reported by previous workers,<sup>2,4</sup> the heat production during polymerization was assumed to be nonuniform, that is, depending on the local temperature and monomer conversion as stated by Eqs. (4)–(6). Temperatures and monomer conversion as a function of time were calculated at intervals of 0.5 mm from the center of the metal prosthesis to the surface of the bone. Figures 15 and 16 show the progress of temperature calculated at the location into the cement that exhibited the highest peak temperature and at the bone–cement interface. The limit for impaired bone regeneration has been suggested to be as low as 50 °C for 1 min exposure.<sup>21,22</sup> Hence, a temperature equal to 50 °C was considered in the present work as the limit temperature for thermal injury of the bone. From results in Figure 16 it is seen that the peak temperature at the bone–cement interface is above the critical temperature for cement thickness higher than 6 mm. Peak temperatures and final monomer conversions in the inner of the cement mantle and at the bone–

cement interface were computed for different thicknesses of cement layer, and the results are depicted in Figure 17. The increase of the peak temperature at the interface is much less pronounced than that in the center because of the relatively high heat capacity of the bone. Furthermore, as a result of the physical properties of the bone, a marked gradient of temperature is observed across the thickness, which, in turn, results in a gradient of final monomer conversion. This is more clearly seen in Figure 18, which shows local monomer conversion across the cement thickness as a function of the dimensionless position. As expected, the monomer conversion increases with the thickness of the cement layer; however, the increase is less marked at the bone–cement interface than in the center. For example, by increasing the thickness of the cement layer from 2 to 8 mm the monomer conversion in the center increases by 40%, and the conversion at the interface increases by 10 %. The use of thinner cement layers has been recommended to reduce the risk of thermal injury. However, it is worth noting that it is accompanied by a higher amount of monomer remaining from the polymerization.

The concern over thermal necrosis of the bone tissue has led some investigators to suggest that freezing the femoral component prior to implantation would reduce the risk of thermal injury. In order to study the influence of prechilling the femoral component on the peak temperature reached at

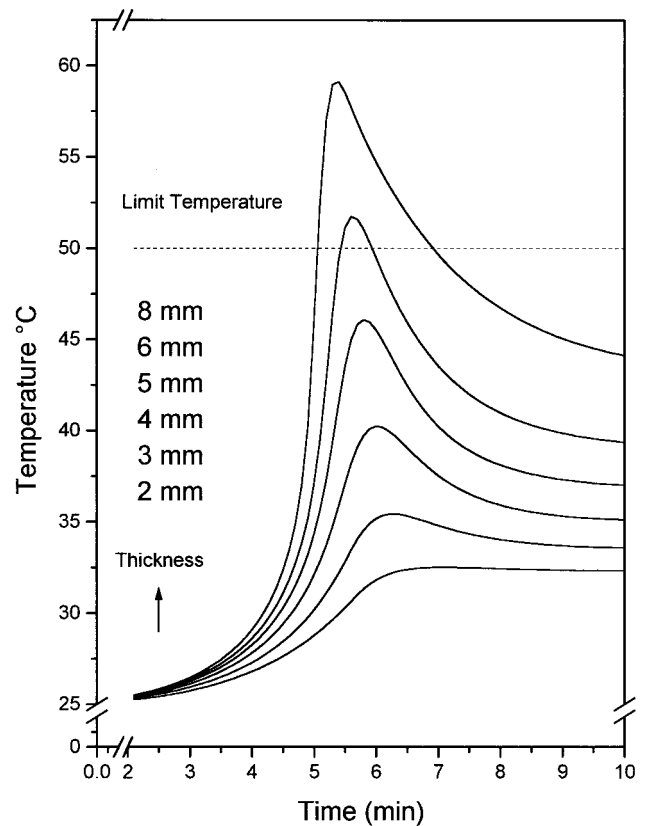


**Figure 16.** Temperature evolution at the bone–cement interface as a function of the cement thickness calculated for the femoral component in a hip replacement. The horizontal line denotes the limit suggested for thermal injury.



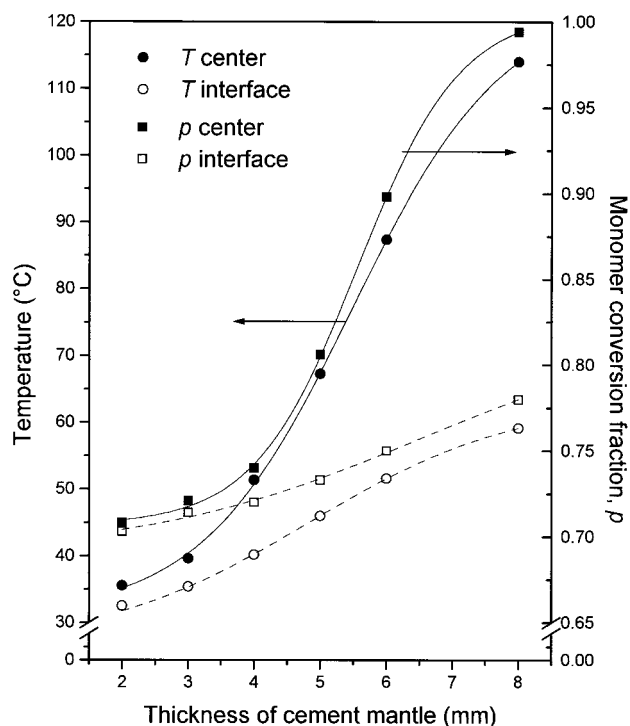


**Figure 17.** Peak temperatures and final monomer conversion fraction calculated in the center of the cement and at the bone–cement interface as a function of the cement thickness.

the bone–cement interface, the initial temperature of the metal stem was set to 5 °C, and the mathematical model was analyzed. Results computed for different initial temperatures of the bone and stem component are outlined in Tables III–VI. For a bone having an initial temperature of 25 °C, prechilling of the stem at 5 °C reduces the peak temperature at the bone–cement interface to values that are below the limit for thermal injury, while the amount of residual monomer is slightly increased. Table V shows that for a bone having an initial temperature of 37 °C the limit temperature is exceeded even for a cement thickness of 5 mm. In this case prechilling of the stem is not an effective means to prevent thermal injury (Table VI). These numerical results are attributed to the relatively high thermal capacity of the bone, which indicates the amount of energy needed to increase its temperature and reveals the importance of reducing the initial temperature of the bone on the peak temperature reached at the bone–cement interface. Cooling of the bone during the surgical procedure results in the reduction of the peak temperature experienced by the bone by about 10 degrees and considerably reduces potential bone necrosis by thermal means. On the other hand, the sink capability of the metal stem may be recognized as an important consideration in implant methodology only in cases when the bone was cooled during the surgical procedures and cement thicknesses higher than 6 mm are required. However, a secondary factor that should be considered when the use of cooled prosthesis is contemplated is that the cement polymerizes with a considerably extended cure time. The polymerization at the

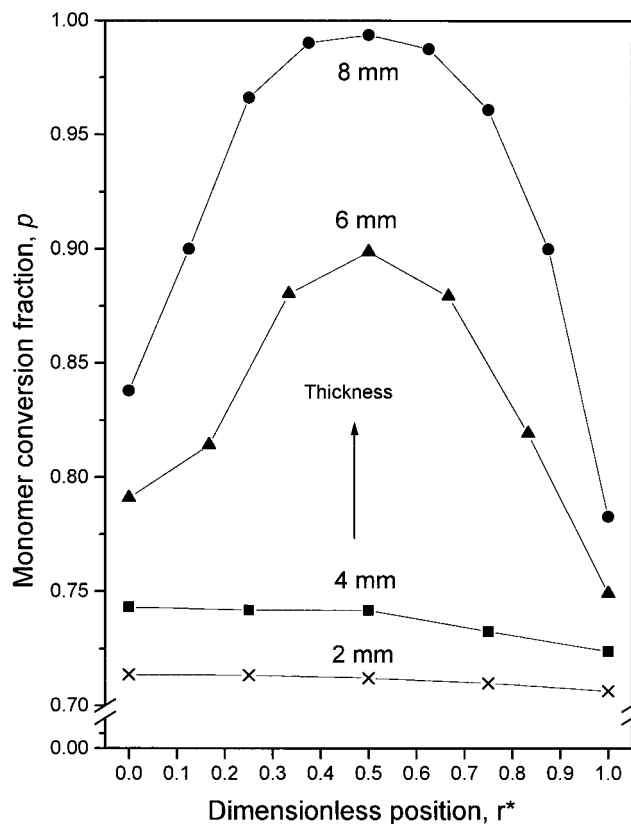


**Figure 18.** Final monomer conversion fraction profiles as a function of the thickness of the cement mantle.  $r^* < 0$  corresponds to the metal–cement interface,  $r^* = 1$  corresponds to the bone–cement interface. The actual position is calculated by  $r^* \times \text{thickness}$ .

bone–cement interface is delayed by about 2 min; therefore, the time for which the bone tissue is exposed to high monomer concentrations is extended.

The influence of the initial temperature of the cement on the temperature and monomer conversion fraction profiles is shown in Figure 19. In practice, these results are valid provided that the mixture is not heated during mixing; that is, the cement is inserted into the bone at a temperature of 4 °C. By chilling the cement at 4 °C prior to cementation the peak temperature is reduced in about 5 °C compared with the value reached for a cement having an initial temperature of 25 °C.

**TABLE III. Peak Temperatures into the Cement and at the Bone–cement Interface. The Initial Temperatures are Bone: 25 °C, Cement: 25 °C, Metal Stem: 25 °C**

Thickness	Peak Temperature (°C)		Monomer Conversion Fraction		
	Cement	Bone–Cement	Metal–Cement	Cement	Bone–Cement
5	71.46	45.80	0.79	0.83	0.73
6	90.21	50.96	0.82	0.91	0.75
7	105.84	54.87	0.85	0.97	0.76
8	116.46	57.57	0.87	1.00	0.78

**TABLE IV. Peak Temperatures into the Cement and at the Bone–Cement Interface. The Initial Temperatures Are Bone: 25 °C, cement: 25°C, Metal Stem: 5 °C**

Thickness	Peak Temperature (°C)		Monomer Conversion Fraction		
	Cement	Bone–Cement	Metal–Cement	Cement	Bone–Cement
5	56.52	39.69	0.76	0.77	0.73
6	72.95	43.92	0.79	0.84	0.74
7	89.60	47.61	0.82	0.92	0.75
8	103.29	50.48	0.85	0.97	0.76

The reduction in the peak temperature is produced without substantial variation in the monomer conversion fraction. Unfortunately, this is accompanied by an extended cure time.

Estimation of the thermal and chemical injury caused by bone cement has been the focus of much research effort. Historically, physical experiments have been performed to measure the temperature at the cement–bone interface with cadaver specimens, with in vitro models, and during joint replacement procedures. Although these studies established important data, the cement mantle could not be varied in a controlled way to note the effect of cement thickness on the measured temperatures. In addition, temperatures were determined only at the specific points where thermocouples were attached. The advantage of the use of a computer model lies in the fact that the temperature–time history can be observed anywhere within the stem–cement–bone model. In addition, the amount of unreacted monomer present in the hardened material may be calculated. The limitations of this approach are attributed to the fact that it makes use of ideal geometry and certain approximations such as the uniformity of the initial temperature of the components (metal stem, cement, and bone).

Further work needs to be performed to establish whether the present findings are formulation specific or have applicability to any acrylic bone cement. Also, additional studies should be conducted on the influence of the incomplete cure on the long-term performance of cemented arthroplasties.

## CONCLUSIONS

A kinetic model for free-radical polymerization has been used to predict the progress of the polymerization of a bone

**TABLE V. Peak Temperatures into the Cement and at the Bone–Cement Interface. The Initial Temperatures Are Bone: 37°C, Cement: 25°C, Metal Stem: 25 °C**

Thickness	Peak Temperature (°C)		Monomer Conversion Fraction		
	Cement	Bone–Cement	Metal–Cement	Cement	Bone–Cement
5	93.46	56.88	0.82	0.91	0.78
6	112.17	60.60	0.85	0.98	0.80
7	123.63	62.63	0.88	1.00	0.81
8	131.79	63.92	0.90	1.00	0.82

**TABLE VI. Peak Temperatures into the Cement and at the Bone–Cement Interface. The Initial Temperatures Are Bone: 37 °C, Cement: 25 °C, Metal-Stem: 5 °C**

Thickness	Peak Temperature (°C)		Monomer Conversion Fraction		
	Cement	Bone–Cement	Metal–Cement	Cement	Bone–Cement
5	71.43	49.40	0.79	0.83	0.76
6	90.81	53.74	0.82	0.92	0.78
7	107.27	56.89	0.84	0.98	0.80
8	118.77	58.98	0.87	1.00	0.81

cement based on PMMA. One of the advantages of this kind of model lies in that it allows one to investigate the effect of process variables such as mold thickness, mold geometry, and mold material on the cure behavior of the cement. Model predictions of the temperature evolution for the batch casting in rectangular and cylindrical molds have shown satisfactory agreement with experimental results. It has been shown that the maximum monomer conversion is conditioned by the cure temperature and the vitrification phenomenon. Because the mold material influences the temperature evolution during the cure of the resin, remarkable differences in the residual monomer content among samples of the same size but cured in molds of different materials are observed.

A mathematical model of hip replacement with varying cement thickness was developed. Theoretical computations

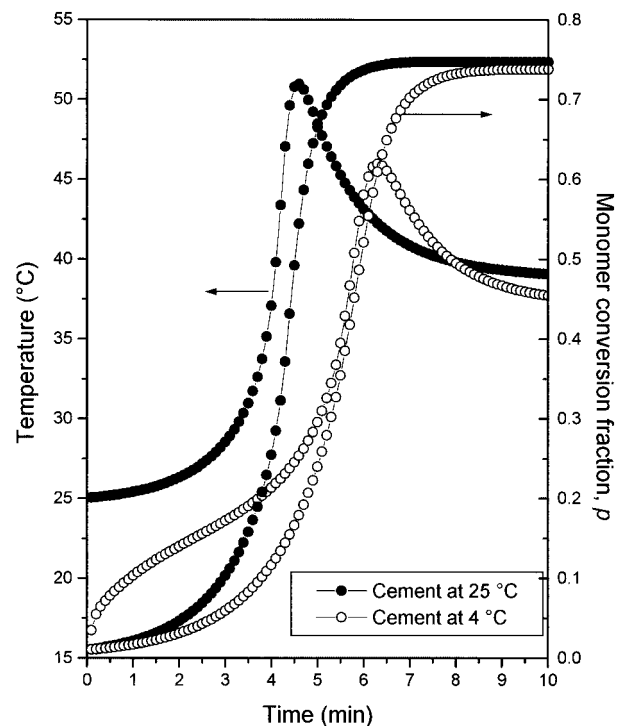


**Figure 19.** Influence of the initial temperature of the cement on temperature and monomer conversion fraction profiles at the bone–cement interface. The cement thickness is 6 mm and the initial temperature of the metal stem and bone is 25 °C.

of the temperature progress indicated that for cement thickness lower than 6 mm the peak temperature at the bone–cement interface was below the reported limit value for thermal injury of the bone. On the other hand, it was shown that the amount of monomer remaining from the polymerization is inversely proportional to the cement thickness.

## REFERENCES

1. Lewis G. Properties of acrylic bone cement: State of the art review. *J Biomed Mater Res Appl Biomater* 1997;38:155–182.
2. Jefferiss CD, Lee AJ, Ling RSM. Thermal aspects of self-curing polymethylmethacrylate. *J Bone Joint Surg Br* 1975;57-B:511–518.
3. Reckling FW, Dillon WL. The bone–cement interface temperature during total joint replacement. *J Bone Joint Surg Am* 1977;59-A:80–82.
4. Swenson LW, Schurman DJ, Piziali RL. Finite element temperature analysis of a total hip replacements and measurement of PMMA curing temperatures. *J Biomed Mater Res* 1981;15:83–96.
5. Schultz RJ, Johnston AD, Krishnamurty S. Thermal effects of polymerization of methyl-methacrylate on small tubular bones. *Inter Orthop* 1987;11:277–282.
6. Harving S, Soballe K, Bünger C. A method for bone–cement interface thermometry. *Acta Orthop Scand* 1991;62:546–548.
7. Toksvig-Larsen S, Franzen H, Ryd L. Cement interface temperature in hip arthroplasty. *Acta Orthop Scand* 1991;62:102–105.
8. Linder LG, Harthorn L, Kullberg L. Monomer leakage from polymerizing acrylic bone cement. *Clin Orthop Relat Res* 1976; 119:242–248.
9. Hailey JL, Turner IG, Miles AW, Price G. The effect of post-curing chemical changes on the mechanical properties of acrylic bone cement. *J Mater Sci Mater Med* 1994; 5:617–621.
10. Vallo CI. Residual Monomer Content in Bone Cements Based on PMMA. *Polymer Internat* 2000;49:831–838.
11. Vallo CI, Cuadrado TR, Frontini PM. Mechanical and fracture behaviour evaluation of commercial acrylic bone cements. *Polymer Int* 1997;43:260–268.
12. Vallo CI, Montemartini PE, Cuadrado TR. Effect of residual monomer content on some properties of a poly(methylmethacrylate)-based bone cement. *J Appl Polymer Sci* 1998;69:1367–1383.
13. Vallo CI. Influence of filler content on static properties of glass-reinforced bone cement. *J Biomed Mater Res Appl Biomater* 2000;53:717–727.
14. Özisic MN, Basic Heat Transfer, McGraw-Hill, New York, 1975.
15. Turi A., editor, Thermal characterization of polymeric materials, Academic, London, 1981.
16. Wang JS, Franzén H, Toksvig-Larsen S, Lidgren L. Does vacuum mixing of bone cement affect heat generation? Analyses of four cement brands. *J Appl Biomater* 1995;6:105–108.
17. De Wijn JR. Reduction of the maximum temperature in the polymerization of cold-and heat-curing acrylic resins. *J Biomed Mater Res* 1974;8:421–434.
18. Clattenberg R, Cohn J. Thermal properties of cancellous bone. *J Biomed Mater Res* 1975;9:169–182.
19. Vachon RI, Walker FJ, Walker DF, Mix GH. In vivo determination of the thermal conductivity of bone using the thermal comparator technique. In Jacobson, B, editor. Digest of the 7th International Conference on Medical and Biological Engineering, 1967.
20. Lundskog J. Heat and bone tissue. An experimental investigation of the thermal properties of bone tissue and threshold levels for thermal injury. *Scand J Plast Reconstr Surg* 1972;9:1–80.
21. Meyers PR, Lautenschlager EP, Moore BK. On the setting properties of acrylic bone cements. *J Bone Joint Surg* 1973; 55:149–156.
22. Eriksson AR, Albrektsson T. Temperature threshold levels for heat induced bone tissue injury: A vital microscopic study in the rabbit. *J Prosthet Dent* 1983;50:101–107.